Stability Enhancement of Multi machine AC Systems by Synchronverter HVDC control

Raouia Aouini, Bogdan Marinescu, Khadija Ben Kilani, Mohamed Elleuch

Stability Enhancement of Multi machine AC Systems by Synchronverter HVDC control

Raouia AOUINI[1], Bogdan MARINESCU[2], Khadija BEN KILANI[1], Mohamed ELLEUCH[1],
[1]Université de Tunis El Manar, ENIT, L.S.E, LR11ES15, BP 37-1002, Tunis le Belvédère, Tunisie,
[2] IRCCyN-Ecole Centrale Nantes, BP 92101, 44321
Nantes Cedex 3, France (e-mail:)
Emails: aaouinii@yahoo.com; bogdan.marinescu@irccyn.ec-nantes.fr
khadija.kilani@enit.utm.tn; Mohamed.elleuch@enit.utm.tn

This paper investigates the impact of the Synchronverter based HVDC control on power system stability. The study considers multi machine power systems, with realistic parameters. A specific tuning method of the parameters of the regulators is used. The proposed control scheme is based on the sensitivity of the poles of the HVDC neighbor zone to the control parameters, and next, on their placement using residues. The transient stability of the HVDC neighbor zone is a priori taken into account at the design stage. The new tuning method is evaluated in comparison with the standard vector control via simulation tests. Extensive tests are performed using Matlab/Simulink implementation of the IEEE 9 bus/3 machines test system. The results prove the superiority of the proposed control to the classic vector control. The synchronverter control allows to improve not only the local performances of the HVDC link, but also the overall transient stability of the AC zone in which the HVDC is inserted.

Keywords: Synchronverter, Synchronous generator/motor, SHVDC, transient stability, damping oscillatory modes.

1. Introduction

High voltage direct current (HVDC) transmission is a mean for transmitting electrical power based on high power electronics, offering thereafter advantages such as transfer capacity enhancement and power flow control [1]. HVDC technology especially the Voltage Source Converter (VSC)-HVDC, stands as a feasible and attractive technology thanks to its controllability and flexibility. Indeed, the VSC technology offers independent control of active and reactive powers, very fast control response, connection of weak systems as offshore wind farms, and black start of isolated systems [2].

HVDC transmission has a wide range of applications. Earlier applications concerned, asynchronous interconnection of AC systems, such as the England-France interconnection [3]. Recently, HVDC links are inserted into complex interconnected AC system in order to improve the grid's transmission capability and flexibility. In this context, the HVDC link co-exists in parallel with other AC system elements. For example, the project Spain-France interconnection [4], which will use the VSC technology, scaled up to 2000 MW.

HVDC is an active technology in the sense that it provides several degrees of freedom for the power and voltage control. Thus, it has an impact on the dynamics of the neighbor AC power system [5]–[15].

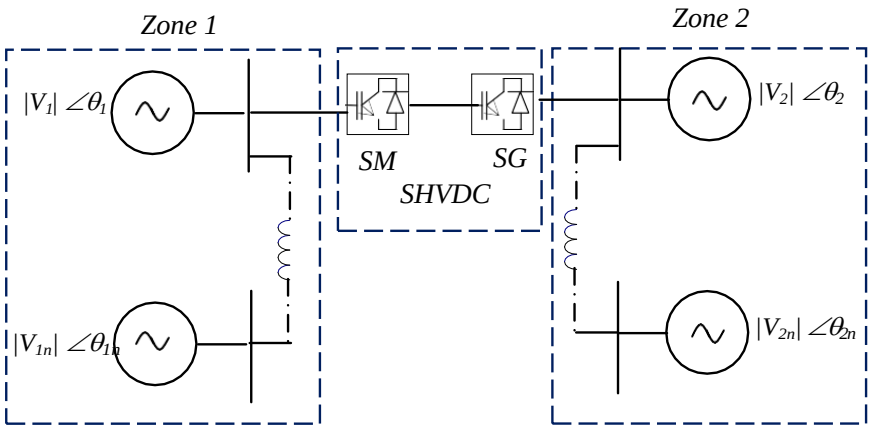

Fig. 1. Schematic of multi machine interconnected by HVDC link

Most control of a VSC-based HVDC system uses a nested-loop *d–q* vector control approach based on the linear PI technology [15]. A novel control concept of power converters labeled "synchronverters" was introduced in [16]. A synchronverter is a converter that mimics the behavior of a synchronous generator (SG) along with its voltage and frequency regulations [16]. Recently in [17], a new control strategy for VSC-HVDC transmission based on the synchronverter concept was proposed. In the HVDC link, the sending-end rectifier emulates a synchronous motor (SM) and the receiving end inverter emulates a synchronous generator (SG). The resulting Synchronverter based HVDC was called SHVDC [17]. The authors developed an analytical method which takes into account, at the tuning stage, the neighboring AC zone of the HVDC link. As a consequence, power system performances were enhanced in addition to local performances.

Nonetheless, the effectiveness of the tuning method of the SHVDC parameters has not been proven for the case of multi machine power systems, with realistic parameters. The model used in [17] considered a two area systems with identical parameters. Such model is not only unrealistic, but also, the results may not be projected to the case of unevenly powered multi machine power system. We therefore propose a more general structure of a multi machine power system, as schematized in Fig. 1.

The proposed model is the full model of the IEEE 3 machine 9 bus benchmark. In the tuning stage, the proposed control technique allows one to take into account dynamic specifications and swing information of the neighbouring AC zones. This design approach ought to provide better dynamic performances and to improve the transient stability of the neighbor AC zone of the HVDC link.

The rest of the paper is organized as follows: in Section 2, the SHVDC structure is recalled. An analytic method to tune the parameters of the controllers of the SHVDC to meet the desired performances is given in Section 3, while validation tests are presented in Section 4.

2. Synchronverter based HVDC

In this Section, the converters of the HVDC line are designed to emulate synchronous machines using the synchronverter concept proposed in [17]. The latter is an inverter which regulations are chosen such that the resulting closed-loop mimics the behavior of a conventional synchronous generator [16]. Therefore, to provide a complete HVDC structure, another synchronverter operating as a synchronous motor (SM) is necessary. As a result, the DC power is sent from the SM to the SG. The resulting system shown in Fig. 2 is called a Synchronverter High-Voltage Direct Current (SHVDC).

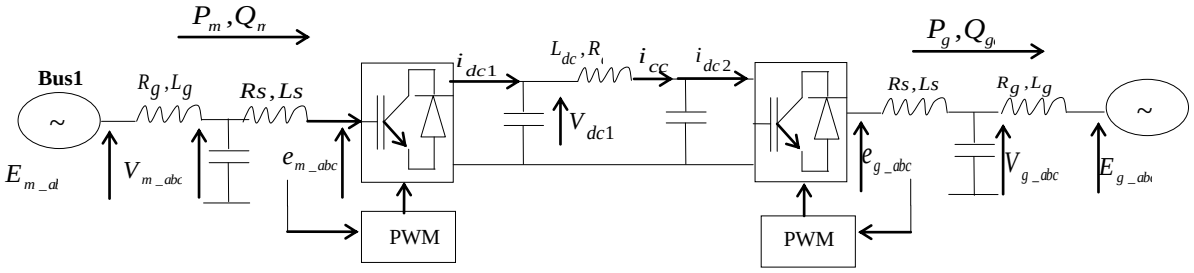

Fig. 1. Two terminal VSC-HVDC link

On Fig. 2, we may depict the following:

(i) the power part of the SG/SM consists of the inverter/rectifier plus an LC filter;

(ii) the controls are assured by the electronic part. VSC converter technologies shown in Fig. 3 are used. The overall structure is shown to be equivalent to an SG/SM with capacitor banks connected in parallel to the stator terminals.

As shown in Fig. 3, the controllers include the mathematical model of a three-phase round-rotor synchronous machine described by the following set of equations:

$$\frac{d\ddot{\theta}_g}{dt} = \frac{1}{J_g}(T_{gm} - T_{em} - D_{gp}\,\mathrm{s}\,\theta_g) \tag{1}$$

$$\frac{d\ddot{\theta}_m}{dt} = \frac{1}{J_m}(T_{mm} - T_{mm} - D_{mp}\,\mathrm{s}\,\theta_m) \tag{2}$$

$$T_{ge} = M_g < i_{g-abc}, \tilde{\sin}\,\theta_g > \tag{3}$$

$$T_{me} = M_m < i_{m-abc}, \tilde{\sin}\,\theta_m > \tag{4}$$

$$e_{g-abc} = M_g s\theta_g \tilde{\sin}\,\theta_g \tag{5}$$

$$e_{m-abc} = M_m s\theta_m \tilde{\sin}\,\theta_m \tag{6}$$

$$P_{ge} = M_g s\theta_g < i_{g-abc}, \tilde{\sin}\,\theta_g > \tag{7}$$

$$P_{me} = M_m s\theta_m < i_{m-abc}, \tilde{\sin}\,\theta_m > \tag{8}$$

$$Q_{ge} = -M_g s\theta_g < i_{g-abc}, \tilde{\cos}\,\theta_g > \tag{9}$$

$$Q_{me} = M_m s\theta_m < i_{m-abc}, \tilde{\cos}\,\theta_m > \tag{10}$$

where

T_{gm} and T_{mm} are the mechanical torques applied respectively to the rotors of the SG and the SM. T_{ge} and T_{me} are the electromagnetic torques applied respectively to the rotors of the SG and the SM. θ is the rotor angle, J_g and J_m are the combined moment of inertia of generator and turbine. s=d/dt is the derivation operator. P_g (respectively P_m) and Q_g (respectively Q_m) are the active and the reactive power, respectively, of the SG (respectively of the SM). M_g and M_m are, respectively, the field excitations of the SG and the SM.

$\tilde{\sin}\,\theta_g$ and $\tilde{\cos}\,\theta_g$ are

$$\tilde{\sin}\,\theta_g = \left[\sin\theta \;\; \sin(\theta - \frac{2\pi}{3}) \;\; \sin(\theta + \frac{2\pi}{3})\right]^T, \tag{11}$$

$$\tilde{\cos}\,\theta_g = \left[\cos\theta \;\; \cos(\theta - \frac{2\pi}{3}) \;\; \cos(\theta + \frac{2\pi}{3})\right]^T. \tag{12}$$

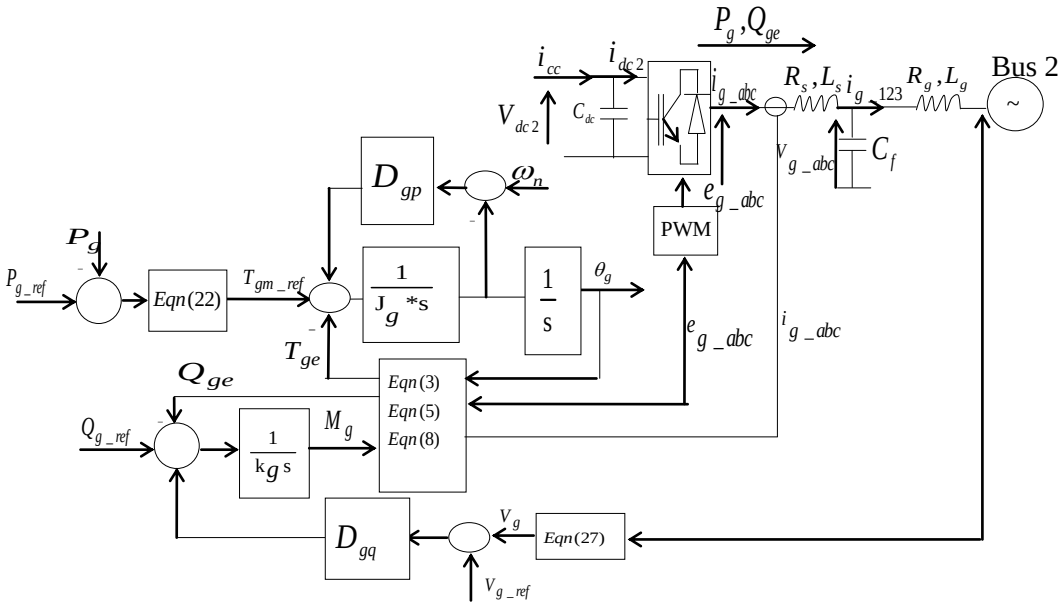

Fig. 2. Model of the synchronverter: power and electronic parts [17]

The operator <.,. > denotes the conventional inner product in R^3.

The phase terminal voltages of the SG and SM are $V_{g\_abc} = [V_{ga}\ V_{gb}\ V_{gc}]^T$, $V_{m\_abc} = [V_{ma}\ V_{gb}\ V_{gc}]^T$ respectively.

$$V_{g\_abc} = -R_s i_{g\_abc} - L_s \frac{di_{g\_abc}}{dt} + e_{g\_abc}, \tag{13}$$

$$V_{m\_abc} = R_s i_{m\_abc} + L_s \frac{di_{m\_abc}}{dt} + e_{m\_abc}. \tag{14}$$

The SHVDC schematized in Fig. 2 is connected to the grid via an impedance (L_g, R_g) such that

$$V_{g\_abc} = \frac{1}{C_f s}(i_{g\_abc} - i_{g\_123}), \tag{15}$$

$$i_{g\_123} = \frac{1}{(R_g + L_g s)}(V_{g\_abc} - E_{g\_abc}), \tag{16}$$

$$V_{m\_abc} = \frac{1}{C_f s}(i_{m\_123} - i_{m\_abc}), \tag{17}$$

$$i_{m\_123} = \frac{1}{(R_g + L_g s)}(E_{m\_abc} - V_{m\_abc}), \tag{18}$$

where $i_{g\_abc} = [i_{ga}\ i_{gb}\ i_{gc}]^T$, $i_{g\_abc} = [i_{ga}\ i_{gb}\ i_{gc}]^T$, are respectively the stator phase currents of the SG and the SM; L_s and R_s are respectively, the inductance and the resistance of the stator windings, and $e_{g\_abc} = [e_{ga}\ e_{gb}\ e_{gc}]^T$, $e_{m\_abc} = [e_{ma}\ e_{mb}\ e_{mc}]^T$ are respectively the back emfs of the SG and the SM.

To emulate the droop of the SG, the following frequency droop control loop is proposed

$$T_{gm} = T_{gm\_ref} + D_{gp}(\omega_n - s\theta_g), \tag{19}$$

$$T_{mm} = T_{mm\_ref} + D_{mp}(\omega_n - s\theta_m). \tag{20}$$

T_{gm_ref} is the mechanical torque applied to the rotor of the SG and it is generated by a PI controller as shown in Fig. 1 to control the real power output P_g. In the SM case, T_{mm_ref} is produced by a DC voltage control for power balance.

$$T_{mm\_ref} = (k_{p\_vdc} + \frac{k_{i\_vdc}}{s})(V_{dc\_ref} - V_{dc1}) \ , \tag{21}$$

$$T_{gm\_ref} = (k_{p\_p_g} + \frac{k_{i\_p_g}}{s})(P_g - P_{g\_ref}) \, . \tag{22}$$

The reactive power Q_{gm} (respectively Q_{mm}) is controlled by a voltage droop control loop using a voltage droop coefficient D_{gq} (respectively D_{mq}), in order to regulate the field excitation M_g (respectively M_m), which is proportional to the voltage generated.

$$M_g = \frac{1}{k_g s}(Q_{gm} - Q_{ge}) \, , \tag{23}$$

$$Q_{gm} = Q_{g\_ref} + D_{gq}(V_{g\_ref} - V_g) \, , \tag{24}$$

$$M_m = \frac{-1}{k_m s}(Q_{mm} - Q_{me}) \, , \tag{25}$$

$$Q_{mm} = Q_{m\_ref} + D_{mq}(V_{m\_ref} - V_m) \, , \tag{26}$$

where V_g (respectively V_m), is the output voltage amplitude is computed by

$$V_g = \frac{2}{\sqrt{3(V_{ga}V_{gb} + V_{ga}V_{gc} + V_{gb}V_{gc})}} \, , \tag{27}$$

$$V_m = \frac{2}{\sqrt{3(V_{ma}V_{mb} + V_{ma}V_{mc} + V_{mb}V_{mc})}} \, . \tag{28}$$

The DC line given in Fig.2 has the following system equations

$$V_{dc1} = \frac{1}{C_{dc} s}(i_{dc1} - i_{cc}) \, , \tag{29}$$

$$V_{dc2} = \frac{1}{C_{dc} s}(i_{cc} - i_{dc2}) \, , \tag{30}$$

$$i_{cc} = \frac{1}{L_{dc} s}(V_{dc1} - V_{dc2} - R_{dc} i_{cc}) \cdot \tag{31}$$

The active power conservation of the AC and the DC circuits gives the following relation

$$P_{dc1} = V_{dc1} i_{dc1} \ , \tag{32}$$

$$P_{dc2} = V_{dc2} i_{dc2} \ , \tag{33}$$

$$P_{dc1} = P_m \ , \tag{34}$$

$$P_{dc2} = P_g \, . \tag{35}$$

3. Control model description

The tuning methodology of the SHVDC parameters developed in [17] is briefly recalled. In order to guarantee the transient stability of the neighbor zone of the HVDC link, neighbor zone dynamics must be taken into account at the design level. Consequently, both the local performances and the transient stability of the neighbor AC systems of the HVDC are enhanced. For this reason, it was necessary to start from a full model of a sufficiently large zone around the HVDC link.

3.1 Control Specifications

The tuning procedure starts by defining the full set of control specifications for a VSC- based HVDC. In order to guarantee the set-points of the transmitted active power, the reactive power and the voltage at the points of coupling, their transient behaviour is tracked with the following transient performance criteria [15, 18]:
-the response time of the active/reactive power is normally in the range of 50 ms to 150 ms;
-the response time for voltage is about 100 ms to 500 ms.

3.2 Control objectives

In our previous work [16], the authors developed a tuning methodology of the SHVDC parameters which takes directly into account; swing information at the synthesis stage for the less damped modes of the neighbor AC zone of the HVDC link. As a consequence, the stability limit in term of the CCT of the neighbor zone was improved in addition to local performances presented above. The local performances for active and reactive power tracking are ensured [16]. In the present work, the formentioned tuning method is adopted for the IEEE 9 bus system. In the context of a multi machine power system, faults are considered at the different machine terminals. The synthesis of the SHVDC parameters must take into account poorly damped oscillations modes. Therefore, both global and local performances are ensured.

3.3 Control Structure

In order to satisfy these control objectives, the open loop system shown in Fig.3 is put into the feedback system structure presented in Fig.4 where H(s) is the linear approximation of the system in Fig.3.
The following diagonal matrix grouped all control parameters

$$K(s,q) = diag(D_{gp}, D_{mp}, K_{p\_Vdc}, K_{i\_Vdc}, D_{gq}, D_{mq}, K_{p\_Pg}, K_{i\_Pg}) \quad (36)$$

where D_{gp}, D_{mp} are, respectively, the static frequency droop coefficients of the SG and the SM; D_{gq}, D_{mq} are, respectively, the voltage droop coefficient of the SG and of the SM; $K_{p\_V_{dc}}, K_{i\_V_{dc}}$ are the DC voltage PI control parameters; and $K_{p\_P_g}$, $K_{i\_P_g}$ are the active power PI control parameters.

Note that all elements of the matrix $K(s,q)$ are tuned via the pole placement presented in Section 3.2.4 to meet HVDC performance specifications given in Section 3.2.1.
The inputs u and the outputs y are

$$u=[T_{mm}, Q_{mm}, T_{mm\_ref\_kp}, T_{mm\_ref\_ki}, T_{gm}, Q_{gm}, T_{gm\_ref\_kp}, T_{gm\_ref\_ki}]^T$$

$$y=[\omega_n - s\theta_m,\ V_{m\_ref} - V_m,\ V_{dc\_ref} - V_{dc},\ \frac{V_{dc\_ref} - V_{dc}}{s},\ \omega_n - s\theta_g,\ V_{g\_ref} - V_g,\ P_{g\_ref} - P_g,\ \frac{P_{g\_ref} - P_g}{s}]^T.$$

3.4 Parameters and residues of the Regulators

The tuning of the control parameters is based on the poles sensitivity to the regulators parameters. Let $H(s)$ be the transfer matrix of a linear approximation of $\tilde{\sum}$ and consider each closed-loop of the feedback system in Fig. 5 which corresponds to the *ith* input *ui and* output *yi* . More specifically, $H_{ii}(s)$ and $K_{ii}(s)$ are the (i,i) transfer functions of *H(s)*, respectively. The sensitivity of a pole λ of the closed-loop in Fig. 2 with respect to a parameter q of the regulator K_{ii} is given by [19]:

$$\frac{\partial \lambda}{\partial q} = r_\lambda \frac{\partial K_{ii}(s,q)}{\partial q} \tag{37}$$

where r_λ is the residue of $H_{ii}(s)$ at pole λ .

Note that, for our case. (36), $\left.\frac{\partial K_{ii}(s,q)}{\partial q}\right|_{s=\lambda} = 1$.

3.5 Coordinated Tuning of SHVDC Parameters

We start by computing the desired locations λ_i^* each pole λ_i defined in the control specifications given in Section 3.2.1. The connections between the dynamics of interest and the modes are established based on the participations factors given in Table 1.

From the same line of Table 1; several dynamics of interest have also significant participations to the same pole which led us to compute the gains K in a coordinated way.

More specifically, if Λ denotes the set indices j from 1 to 8 for which $H_{jj}(s)$ has λ_i as pole, the contribution of each control gain in the shift of the pole is

$$\lambda_i = \lambda_i^0 + \sum_{j \in \Lambda} r_{ij} K_j \ , \tag{38}$$

where λ_i^0 is the initial location (open-loop) of the pole λ_i and r_{ij} is the residue of $H_{jj}(s)$ in λ_i . Finally, the pole placement is the solution of the following optimization problem

$$\{K_j^*, j = 1...8\} = \arg\min_{K_j} \sum_i \left\| \lambda_i^* - \lambda_i \right\|^2 \ , \tag{39}$$

where λ_i is given by (38).

The optimal parameters in the appendix were obtained with (39) solved for the desired locations in Table 1. The specific tuning SHVDC parameters are tested on the IEEE 9 bus/3 machines benchmark [20] shown in Fig. 3.

4. Simulations Results

The considered case is the IEEE WSCC 9-bus test power system, which represents a simple approximation of the Western System Coordinating Council (WSCC). The model contains 3 generators, 3 loads, 5 branches and 3 two-winding power transformers, as illustrated in Fig. 6. The line between buses 4 and 5 is replaced by an HVDC transmission line. The HVDC link is 100 km long, has a rated power of 200 MW and a DC voltage rating of ±100 kV [20]. Each of the units is connected through transformers to the 100 kV transmission line. The ratings of each generator are 600 MVA and 20 kV. The detailed system data is given in the appendix. The loads L_1 , L_2 and L_3 are modeled as constant impedances. The simulations performed are intended to test the performances and robustness of the proposed control. Simulations tests use Matlab/Simulink toolbox.

4.1 HVDC-VSC vector control

Usually, the main trends in control techniques for HVDC- VSC links are based on the well-established vector control scheme. The two converters are controlled by two independent loops and each of these controls is based on the vector control approach in the d-q frame, using cascaded PI controllers [15]: the outer control loop generates the respective d-q current references to the inner current control loop. The tuned SHVDC parameters technique presented in the previous Section is tested and compared with the classic vector control. The two controllers are tuned to satisfy the same performance specifications (the usual time setting for HVDC voltage and power control presented in

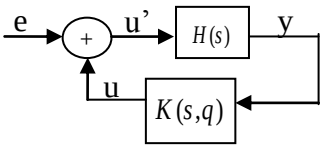

Fig. 4. Feedback system

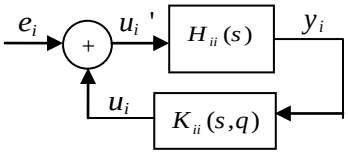

Fig. 5. Single input/Single output feedback system

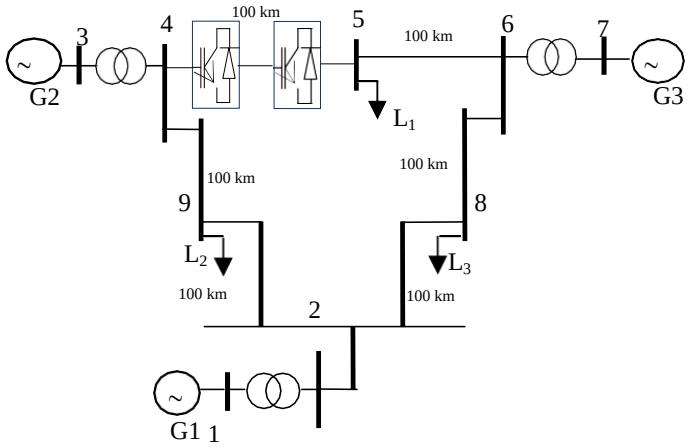

Fig. 6. IEEE 9 bus system

***Table 1*:** Desired modes meeting the HVDC specifications

Dynamics of interest	λ_i^o	λ_i^*	$r_{\lambda_i^o}$
Voltage V_m	-5.36	-10	-0.18
Voltage V_g	0.035	-10	-0.12
Active Power P_m	1.69±5.07i	-21±21.42i	-0.08 ±0.06i
	-2.78±18.89	-21±21.42i	-0.02 ±0.07i
	-2.57±3.51	-11±10i	-0.05 ±0.08i
	0.2±0.604i	-13±14i	-0.2 ±0.33i
Active Power P_g	-0.23±4.405	-21±21.42i	-0.15 ±0.002i
	0.001	-50	0.29
Reactive Power Q_m	-5.36	-10	-0.18
Reactive Power Q_g	0.035	-10	-0.12

Section 3.1).

4.1 Local performances

Table 1 (column 3) presents the desired location of modes λ_i^* for each dynamic of interest. The optimal parameters K in the appendix was obtained with (39) solved for the desired locations in Table 1. The response of SHVDC for the test power system in Fig. 3 with these tuned parameters is given in Fig. 6 in solid lines in comparison with the ones in dotted lines obtained with a classic vector control. Figs 6.a and 6.b show the responses of active and reactive powers to a +0.1 p.u step in P_{g_ref} and to a -0.1 p.u step in $Q_{g\_ref..}$ A good tracking of the active power reference and satisfying control specifications for both responses is observed. It is noted that better dynamic responses are provided with the SHVDC coordinated controller.

4.2. Transient stability

Fig. 9.a, b and c, respectively show the responses of the angular speed of generator G1, G2 and G3 of the benchmark in Fig. 6 to a three phase short circuit fault of 100 ms. The figure depicts better dynamic responses with the SHVDC coordinated controller. The simulation responses show that the transient oscillations obtained with the new controller are more damped than the ones obtained with the standard vector control.

The transient stability margin of the power system is estimated by the Critical Clearing Time (CCT) which is defined as the maximal fault duration for which the system remains transiently stable [21]. The instability is then manifested by the loss of synchronism of a group of machines. In addition to the previous simulations, the CCT obtained with the SHVDC controller were compared to the ones obtained with the standard control. The obtained CCTs for a three-phase short-circuit occurring near each generator are presented in Table 2 for the classic vector control, and the proposed SHVDC control. We can see that the SHVDC control with tuned parameters improves the transient dynamics of the system and thus augments the transient stability margins of the neighbor network. This is due to the fact that the dynamics of the neighbour zone are taken into account at the synthesis stage via the oscillatory modes in Table 1. The gains of the controllers are computed to damp these modes and thus to diminish the general swing of the zone and not only for the local HVDC dynamics.

4.4 Tests of Robustness

Robustness of the proposed controller is tested for initial condition and for power flow change in direction. Since the synthesis of the SHVDC controller is based on linear approximation, robustness of performances against the variation of the operating point is required. Therefore, a new load flow setting is considered for the simulations. For example, the active power of load L1 is increased by 50 MW. The gains of the SHVDC controller are not recomputed and are thus the same as in the appendix. Fig. 9 gives the active power response to +0.1 step in $P_{g\_ref.}$ The latter is comparable with the one obtained in Fig. 6.a.

(a) (b)

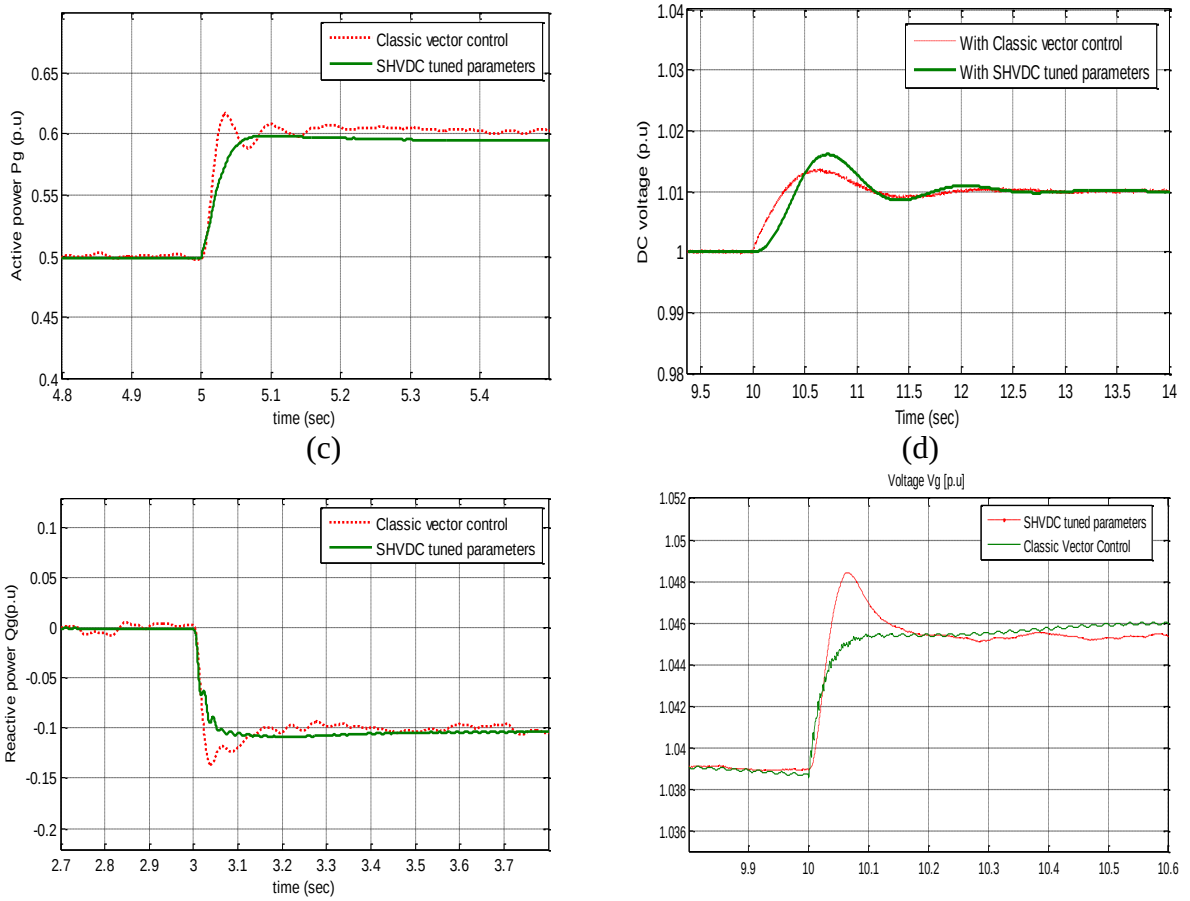

(a)Response of P_g to a +0.1 step in P_{g_ref} (p.u)
(b) Response of V_{dc} to a +0.1 step in V_{dc_ref} (p.u)
(c)Response of Q_g to a -0.1 step in Q_{g_ref} (p.u)
(d)Response of V_g to a +0.1 step in Q_{g_ref} (p.u)

Fig.6. Local performances of the IEEE 9 bus system

(a) (b)

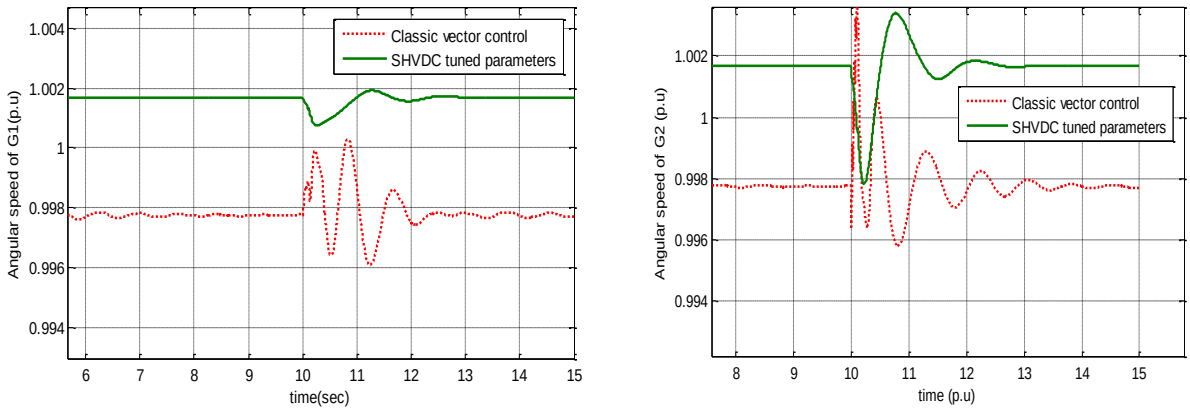

(c)

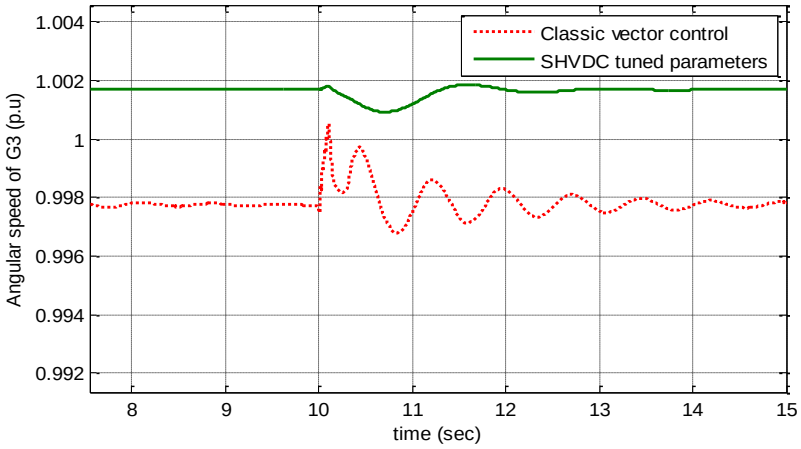

Fig.8. Responses of the angular speed to a 100 ms short circuit near to G2
(a)Angular speed of G1 (p.u)
(b)Angular speed of G2 (p.u)
(c)Angular speed of G3 (p.u)

Table 2: Critical Clearing Times with both control strategies

CCT (ms)	**G1**	**G2**	**G3**
SHVDC	250	200	200
Vector control	150	120	150

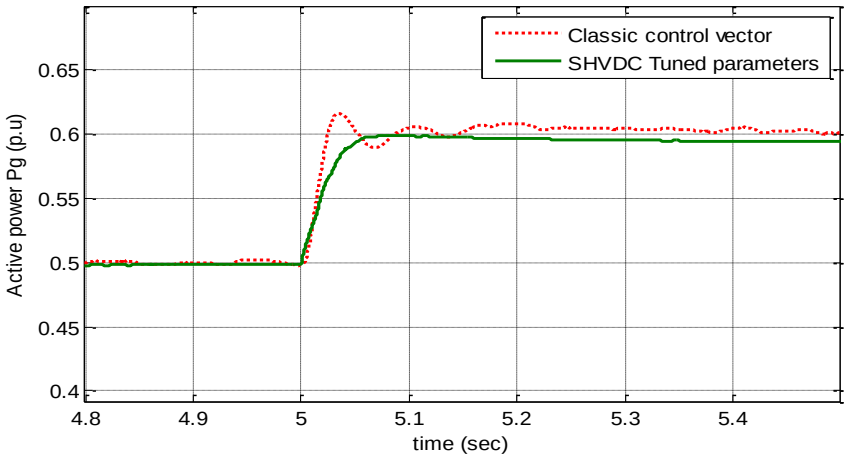

Fig.9. Response of P_g to a +0.1 step in P_{g_ref} (p.u) with a new operating point

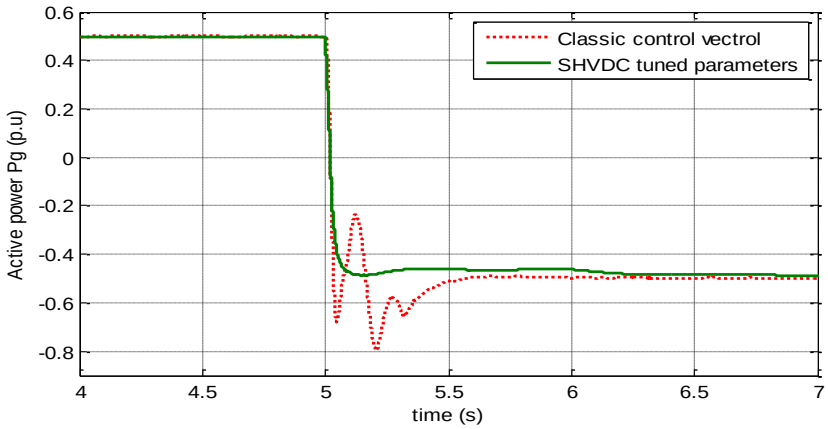

Fig.10. Response of P_g to a -0.5 step in P_{g_ref} (p.u)

Furthermore, the performances of the controller to a sudden change in the direction of the transmitted power are tested by applying a step of -0.5 p.u in P_{g_ref}. Fig. 10 shows that change in power flow direction has no effect on the SHVDC performances. These results confirm the good robustness of the proposed controller against variation of operating conditions.

5. Conclusion

This paper proposed a method for improving the stability of multi machine power system by means of synchronverter based controls of HVDC links. A realistic power system model was used: the IEEE WSCC 3-machine 9-bus benchmark in which an HVDC link was introduced. The transient stability of the HVDC neighbor zone has been taken into account at the design stage of the controller. The proposed control scheme is based on the sensitivity of the poles of the HVDC neighbor zone to control parameters, and on their placement using residues.

The results prove the superiority of the proposed control to the classic vector control. The synchronverter control allows to improve not only the local performances of the HVDC link, but also the overall transient stability of the AC zone in which the HVDC is inserted:

- Better dynamic performance in terms of reduced overshoot and damped oscillatory responses. Indeed, the proposed control design allows one to analytically take into account dynamic specifications at the tuning stage.

- Better stability margin of the neighbor zone, swing information is directly taken into account at the synthesis stage in terms of the less damped modes of the neighbor zone and not only for the local HVDC dynamics as it is the case for the standard VSC control.

- Good robustness of the proposed controller against variation of operating conditions: load change, power flow change in direction.

The exploitation of the proposed control in multi machine applications may be more advantageous when the connected systems present special dynamics, such as renewable generators, weekly connected systems, and systems with week inertia.

6. References

[1] Bahrman, M.P.; Johnson, B.K. The ABCs of HVDC transmission technologies, *IEEE Power and Energy Magazine*, Vol. 5, No. 2, 2007.

[2] Flourentzou, N.; Agelidis, V.G.; Demetriades, G.D. VSC-Based HVDC Power Transmission Systems: An Overview, *IEEE Transactions on Power Electronics*, Vol. 24, No. 3, 2009.

[3] F. Goodrich and B. Andersen, The 2000 MW HVDC link between England and France. *Power Engineering Journal* Vol. 1, No. 2, pp 69-74, 1987.

[4] Y. Decoeur, “France-Spain interconnections, first step for smart grids,” Inelfe. Madrid, Spain, Mar. 26th, 2012.

[5] Hauer, J.F.: ‘Robustness issues in stability control of large electric power systems’. Proc. 32nd IEEE Conf. on Decision and Control, 1993, pp. 2329–2334.

[6] Vovos, N.A., Galanos, G.D.: ‘Enhancement of the transient stability of integrated AC/DC systems using active and reactive power modulation’, *IEEE Power Eng. Rev*.., 1985, 5, (7), pp. 33–34.

[7] Smed, T., Andersson, G.: ‘Utilizing HVDC to damp power oscillations’, *IEEE Trans. Power Deliv*., 1993, 8, (2), pp. 620–627

[8] Hammad, A.E., Gagnon, J., McCallum, D.: ‘Improving the dynamic performance of a complex AC/DC system by HVDC control modifications’, *IEEE Trans. Power Deliv*., 1990, 5, (4), pp. 1934–1943

[9] Shun, F.L., Muhamad, R., Srivastava, K., Cole, S., Hertem, D.V., Belmans, R.: ‘Influence of VSC HVDC on transient stability: Case study of the Belgian grid’. Proc. IEEE Power and Energy Society General Meeting, 25–29 July 2010, pp. 1–7

[10] Taylor, C.W., Lefebvre, S.: ‘HVDC controls for system dynamic performance’, *IEEE Trans. Power Syst*., 1991, 6, (2), pp. 743–752

[11] Latorre, H.F., Ghandhari, M., Söder, L.: ‘Control of a VSC-HVDC operating in parallel with AC transmission lines’. Proc. Transmission and Distribution Conf. and Exposition IEEE, Latin America, 2006, pp. 1–5

[12] Henry, S., Despouys, O., Adapa, R., et al.: ‘Influence of embedded HVDC transmission on system security and AC network performance’. Cigré, 2013

[13] To, K., David, A., Hammad, A.: ‘A robust co-ordinated control scheme for HVDC transmission with parallel AC systems’, *IEEE Trans. Power Deliv*., 1994, 9, (3), pp. 1710–1716

[14] Latorre, H., Ghandhari, M.: ‘Improvement of power system stability by using a VSC-HVDC’, *Int. J. Electr. Power Energy Syst*., 2011, 33, (2), pp. 332–339.

[15] S. Li, T.A. Haskew, and L. Xu, , "Control of HVDC light system using conventional and direct current vector control approaches," *IEEE Trans. Power Syst*., 2010, 25, (12), pp. 3106–3118.

[16] Q.-C. Zhong, and G.Weiss, "Synchronverters: Inverters that mimic synchronous generators," *IEEE Trans. Ind. Electron*., Apr. 2011, vol. 58, no. 4, pp. 1259–126.

[17] R. Aouini, B. Marinescu, K. Ben Kilani and M. Elleuch" Synchronverter-based Emulation and Control of HVDC transmission," *IEEE Trans. Power Syst*., Jan. 2016, Vol. 31, Issue: 1 Pages: 278 – 286.

[18] M-K-S. Sangathan, J- Nehru "Performance of high-voltage direct Current (HVDC) systems with Line- commutated converters", bureau of find Indian standard Manak Bhavan, 9 Bahadur Shah Zafar Marg New Delhi 110002 , April 2013.

[19] G. Rogers, "Power System Oscillations", Kluwer Academic, 2000.

[20] jaikumar Pettikkattil, Simulink Model of IEEE 9 Bus System with load flow, Matlab file ,18 Mar 2014.

P. Kundur, "Power system stability and control", Mc Graw-HillInc, 1994.

7. Appendix

K= [55; 46.4; 24.0 ; 28.5 ; 65.64; 58.069; 56.39; 25.11; 37.35].
Parameters of the classic vector control: current loop: kp= 0.6, ki=8, reactive power control: ki=10, active power control: ki=10, DC voltage control: kp=10, ki=10.

Generators: Rated 600 MVA, 20 kV
Xl (p.u): leakage Reactance = 0.18, Xd (p.u.): d-axis synchronous reactance = 1.305, T’d0 (s): d-axis open circuit sub-transient time constant =0.296, T'_{d0} (s): d-axis open circuit transient time constant = 1.01 ; Xq (p.u): q-axis synchronous reactance = 0.053, Xq (p.u): q-axis synchronous reactance = 0.474, X’’q (p.u): q-axis sub-transient reactance =0.243, T’’q0 (s): q-axis open circuit sub transient time constant=0.1. M =2H (s): Mechanical starting time = 6.4.
Governor control system : R (%): permanent droop =5, servo-motor: ka = 10/3, ta (s) = 0.07, regulation PID: kp = 1.163, ki= 0.105, kd= 0.
Excitation control system : Amplifier gain: ka = 200, amplifier time constant: Ta (s) = 0.001, damping filter gain kf = 0.001, time constant te (s) = 0.1.
27th AC filter in AC system 1 & 2: reactive power=18 MVAR, tuning frequency=1620 Hz, quality factor=15. 54th AC filter in AC system 1 & 2: reactive power=22 MVAR, tuning frequency=3240 Hz, quality factor=15.
DC system: voltage= ±100 kV, rated DC power=200 MW, Pi line R=0.0139 Ω /km, L=159
µH/km, C=0.331 µF/km, Pi line length= 150 km, switching frequency=1620 Hz, DC capacitor=70 µF, smoothing reactor: R=0.0251Ω , L= 8mH.
Loads: PL1=300 MW, PL2= 300 MW ; PL2= 300 MW
AC transmission lines: Resistance per phase (Ω/km) =0.03, Inductance per phase (mH/km)
=0.32, Capacitance per phase (nF/km) =11.5.